Simplified modelling of full-strain-range non-linearity of cyclically loaded undrained clays

Maosong Huang[1,2#], *He* Cui[1,2], *Zhenhao* Shi[1,2], and *Jian* Yu[1,2]

[1] *Key Laboratory of Geotechnical and Underground Engineering of Ministry of Education, Tongji University, China*
[2] *Department of Geotechnical Engineering, Tongji University, China*
[#]*Corresponding author: mshuang@tongji.edu.cn*

ABSTRACT

Constitutive modelling of cyclically loaded undrained clay is of significant importance for various branches of geotechnical engineering exemplified by offshore wind turbine (OWT) foundation design and prevention and mitigation of earthquake hazards. Fine-grained soils can display non-linear stress-strain relations from small (10^{-5}) to relatively large (10^{-1}) strain levels. This full-strain-range non-linearity can remarkably affect the cyclic response. Effective stress-based constitutive models have achieved great success in modelling clayey soils, whereas they can be overly complex for practicing engineers, in particular, when considering non-monotonic loading and full-strain-range non-linearity. This paper explores the possibility of modelling, in simplified manner, the full-strain-range nonlinearity of cyclically loaded undrained clay, which can directly utilize outcomes of in situ site exploration and routine laboratory tests. For this purpose, we idealize soils under undrained conditions as single-phase materials governed by total stress. Considering that most current total stress-based models are proposed for metals and may be limited to capture the non-linear stress-strain relations of soil, a novel generalized non-linear (GNL) hardening law is proposed that can describe versatile stress-strain relations of undrained clays. Bounding surface and a mapping rule considering update of projection centre are introduced to reflect the influences of maximum past stress history and recent stress history, respectively, on the stress-strain nonlinearity. The simplified constitutive model is first validated at the element level by simulating monotonic and cyclic loading laboratory tests on undrained clays. Later, the proposed soil model is applied to the finite element analyses of OWT pile foundation subjected to cyclic lateral loading.

Keywords: Undrained clay; Cyclic loading; Constitutive relations; Nonlinear hardening.

1. Introduction

Many offshore wind turbine (OWT) farms are constructed or planned in sea areas, of which the foundation soils are mainly fine-grained soils such as clay (Byrne et al. 2020; Liu et al. 2020). Due to the low permeability, soils around the OWT foundation are usually assumed in undrained condition. For foundations supporting offshore wind turbines (e.g., monopile foundation) under long term cyclic loading due to wind, current, and tide actions (Nanda et al. 2017; Achmus et al. 2009; Bourgeois et al. 2010), cyclic degradation of soil strength and stiffness may cause cumulative foundation tilt exceeding the serviceability limit state (SLS). Furthermore, fine-grained soils can display non-linear stress-strain relations from small (10^{-5}) to relatively large (10^{-1}) strain levels, and the full-strain-range non-linearity of clay can remarkably affect the cyclic response of foundation (Zhu et al. 2022; Zhang et al. 2017; Hong et al. 2017). To represent the behaviour of undrained clay under cyclic loading, multiple effective stress-based constitutive models have been proposed and achieved considerable success (Seidalinov and Taiebat 2014; Shi et al. 2018). However, they may be over complicated when considering non-monotonic loading condition and have difficulty in calibrating model parameters by simply utilizing data from laboratory or in situ experiment tests.

It is noting that total stress-based model assuming the undrained clay as single-phase material can reasonably describe the monotonic and cyclic loaded response of fine-grained soil (Anastasopoulos et al. 2011; Kourkoulis et al. 2014; Krabbenhøft et al. 2019; Whyte et al. 2020; Huang et al. 2021). In addition to the advantage of operating directly on laboratory and in situ soil characteristic parameters (e.g., undrained shear strength from T-bar tests), total stress-based model can also reasonably represent the hysteretic behaviour of undrained clay by introducing nonlinear hardening rule and bounding surface plasticity, as well as the degradation of stiffness and strength of undrained clay. Nevertheless, as most of existing total stress models were proposed initially for metals, their ability to capture stress-strain non-linearity unique to soils can be limited.

In this paper, a total stress-based model is proposed for cyclic loaded undrained clay. A novel generalized non-linear (GNL) hardening law is proposed that can describe versatile stress-strain relations of undrained clays. Bounding surface plasticity and a mapping rule considering update of projection centre are introduced to describe the hysteretic behaviour of soil during cyclic loading. The simplified constitutive model is first validated at the element level by simulating monotonic

and cyclic loading laboratory tests on undrained clays. Later, the proposed soil model is applied to the finite element analyses of OWT pile foundation subjected to cyclic lateral loading.

2. Model formulation

In many built and planned OWT farms, fine-grained soils constitute the primary sea-bed (Houlsby et al. 2005; Liu et al. 2020). Given the low permeability of the clayey soils, undrained conditions are often assumed for soil around monopile foundation under cyclic loading. This study idealizes undrained clay as a single-phase material governed by total stresses. The formulation of the total stress model will be briefly described in this section.

The employed total stress-based soil model can capture the cyclic degradation of the stiffness and strength of undrained clay. In addition, a novel generalized non-linear (GNL) hardening law is proposed that can describe versatile stress-strain relations of undrained clays.

2.1. Basics of model

The proposed model employs a Mises type bounding surface (see $f = 0$ in Fig. 1):

$$f = \sqrt{\frac{3}{2}\bar{S}_{ij}\bar{S}_{ij}} - \kappa R = 0 \tag{1}$$

where $\bar{S}_{ij}$ indicates the image stress on the bounding surface, R denotes the radius of the strength surface (e.g., for isotropic strength condition, $R=2s_u$), while κ indicates the ratio between the size of the bounding surface and strength surface (i.e., when $\kappa=1$, the bounding surface coincides with the strength surface).

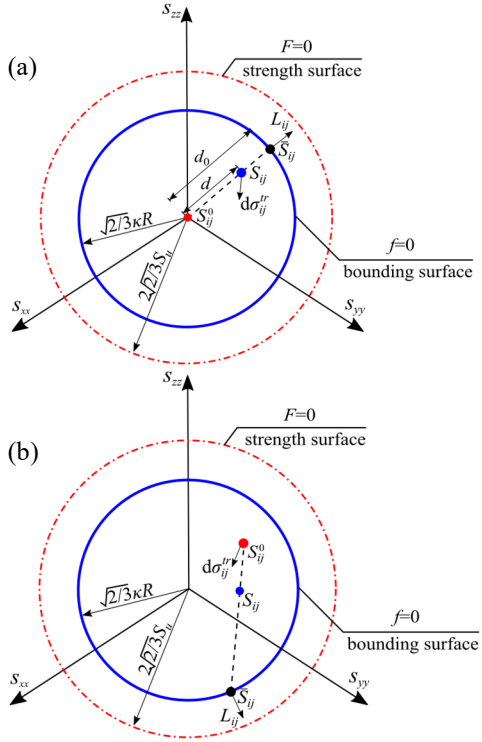

Figure 1. Schematics illustrating bounding surface $f = 0$, strength surface $F = 0$, mapping rule and moving projection center: (a) trigger update of projection center; (b) after update of projection center.

2.2. Generalized non-linear (GNL) hardening rule

Based on typical non-linear hardening rule, the evolution of the hardening parameter κ might be described as:

$$d\kappa = \gamma d\varepsilon_d^p - \gamma\kappa d\varepsilon_d^p \tag{2}$$

where $d\varepsilon_d^p$ denotes the deviatoric plastic strain increment, while γ is a constant material parameter. The first item represents the linear hardening part, and the second item denotes the non-linear part (since it depends on the current value of κ).

By integrating Eq. (2), the hardening equation can be expressed as the follows:

$$\kappa = 1 - \exp(-\gamma\varepsilon_d^p) \tag{3}$$

As shown in Eq. (3), with the increase of ε_d^p, κ tends to 1 exponentially. Although the form of Eq. (3) is simple, yet the form of the stress-strain is relatively fixed. Therefore, the proposed model improves the expression by introducing a shape parameter n, as show in Eq. (4):

$$\kappa = 1 - \exp\left(-\gamma\left(\varepsilon_d^p\right)^n\right) \tag{4}$$

Equation (4) shows that the form of the stress-strain relation can be adjusted more flexibly by change the value of n (i.e., the concept of generalized non-linear (GNL) hardening rule proposed in this paper). Therefore, the evolution of hardening parameter κ can be rewritten as follows by differentiating Eq. (4):

$$d\kappa = n\left(\varepsilon_d^p\right)^{n-1}\gamma\left(1-\kappa\right)d\varepsilon_d^p \tag{5}$$

It can be seen from Eq. (5) that when $\kappa=1$ (i.e., the current deviatoric stress reaches the peak deviatoric stress R), the increment $d\kappa$ is equal to zero that indicates the termination of the hardening of the bounding surface.

2.3. Bounding surface formulation

As shown in Fig.1, the image stress is determined through a mapping rule (Dafalias 1986):

$$\bar{S}_{ij} = b\left(S_{ij} - S_{ij}^0\right) + S_{ij}^0 \tag{6}$$

where S_{ij} is the deviatoric stress ($S_{ij}=\sigma_{ij}-\sigma_{mm}/3\delta_{ij}$, where δ_{ij} is the Kronecker delta and obeys the Einstein summation convention: $\sigma_{mm}=\sigma_{11}+\sigma_{22}+\sigma_{33}$); S_{ij}^0 denotes the projection center that maps the current deviatoric stress S_{ij} radially on the bounding surface to obtain image stress $\bar{S}_{ij}$; while b denotes the ratio between Euclidian distance between the projection center and the image stress (d_0 in Fig. 1 (a)) over that between the projection center and the current deviatoric stress (d in Fig. 1 (a)).

Based on the interpolation parameter b, the plastic modulus K_p can be determined from the following interpolation function:

$$K_p = \bar{K}_p + \mu R\left(b^w - 1\right) \tag{7}$$

where μ and ψ are material constants, while $\bar{K}_p$ denotes the plastic modulus corresponding to the image stress on the bounding surface.

In particular, the location of the projection center will update once the stress reversal occurs (see Fig. 1(b)). The judgement criteria can be established by calculating the angle between the trial elastic stress increment and the loading direction (i.e., the gradient of the bounding surface at the image stress):

$$\frac{\partial f / \partial \bar{\sigma}_{ij} \mathrm{d}\sigma_{ij}^{tr}}{\left\| \partial f / \partial \bar{\sigma}_{ij} \right\| \left\| \mathrm{d}\sigma_{ij}^{tr} \right\|} \le -TOL \tag{8}$$

where $\mathrm{d}\sigma_{ij}^{tr}$ is the trial elastic stress increment, while TOL indicates an error tolerance of relative small value.

2.4. Cyclic softening effects

To consider the deterioration of the strength and stiffness of undrained clay under cyclic loading, a softening relationship is proposed in this model referring the degradation relation proposed by Einav and Randolph (2005), as all parameters required can be obtained from in situ tests (e.g. T-bar test):

$$\frac{R}{R_0} = \delta_{rem} + \left(1 - \delta_{rem}\right) \exp\left(-\frac{3\varepsilon_d^p}{\varepsilon_{95}^p} \right) \tag{9}$$

where R and R_0 denote the softened and initial size of the strength surface, δ_{rem} is the ratio of s_u / s_{u0} that corresponds to a fully remolded state, and the material constant ε_{95}^p indicates the required plastic shear strains to cause 95% reduction of soil undrained strength. Furthermore, the parameters related to deterioration of soil stiffness (i.e., μ and G_0) can also be expressed in a similar form:

$$\frac{\mu}{\mu_0} = \delta_{rem}^e + \left(1 - \delta_{rem}^e\right) \exp\left(-\frac{3\varepsilon_d^p}{\varepsilon_{e95}^p} \right)$$

$$\frac{G_0}{G_0^{ori}} = \delta_{rem}^e + \left(1 - \delta_{rem}^e\right) \exp\left(-\frac{3\varepsilon_d^p}{\varepsilon_{e95}^p} \right) \tag{10}$$

where μ_0 and G_0^{ori} represent the initial value of μ and G_0, respectively, and constant material parameters δ_{rem}^e and ε_{e95}^p control the speed of the reduction of soil stiffness.

2.5. Elastic response

The elastic response of undrained clay is described by a simple isotropic elastic model that includes shear modulus at very small strains G_0 and Poisson's ratio v as parameters. The parameter G_0 can be determined with the following equation:

$$G_0 = G_0^{ref} \left(\frac{p_c'}{p_{ref}} \right)^{n_g} \tag{11}$$

where G_0^{ref} and n_g are material constants, p_c' is the mean effective stress of soil after consolidation, while p_{ref} denotes the reference stress of which the value is 100kPa by default.

The elastic modulus D_{ijkl}^e can be derived with the volume modulus K_t and parameter G_0 within the range of isotropic elastic model as follows:

$$D_{ijkl}^e = \left(K_t - \frac{2G_0}{3} \right) \delta_{ij}\delta_{kl} + 2G_0 \delta_{ik}\delta_{jl} \tag{12}$$

where $K_t = 2(1+v)/3(1-2v)\, G_0$.

3. Performance of GNL hardening law

Except for considering non-monotonic loading condition, the proposed constitutive model may flexibly describe multiple stress-strain relationships of undrained clay owing to the generalized non-linear (GNL) hardening law. The evaluation of the proposed model on approximating typical stress-strain relationship will be performed, and the influence of the generalized non-linear (GNL) hardening rule on the form of stress-strain curves will also be assessed in this section.

To assess the performance of the proposed model on representing typical stress-stain relations of soils, hyperbolic stress-strain response is selected as an example in this paper. Hyperbolic stress-strain response is a widely used form for describing the hardening law of undrained clay (Kondner 1963; Hardin 1978; Subramaniam and Banerjee 2013), and a universal hyperbolic equation can be expressed as:

$$q = \frac{E_i \varepsilon_d}{1 + E_i \varepsilon_d / q_a} \tag{13}$$

where q denotes the deviatoric stress, $q_a = R/R_f$, R denotes the peak deviatoric stress, R_f represents the failure ratio, while E_i indicates the initial elastic modulus. Considering that the elastic deviatoric strain $\varepsilon_d^e = q/E_i$, the relationship between the plastic deviatoric strain ε_d^p and mobilized shear strength coefficient M ($M = q/R$) can be expressed by:

$$\varepsilon_d^p = \frac{R}{E_i} \left(\frac{M}{1 - MR_f} - M \right) \tag{14}$$

By assuming that the current deviatoric stress coincides with the image stress, the counterpart relation based on the proposed model (i.e., Eq. (4)) can be written as follows:

$$M = \frac{q}{R} = 1 - \exp\left(-\gamma \left(\varepsilon_d^p \right)^n \right) \tag{15}$$

To coincide with the form of hyperbolic response, the deviatoric plastic strains corresponding to 50% and 95% of the undrained strength is further assumed to be the same for the two different hardening rule equations. By substituting q=0.5R and q=0.95R into Eq. (14), the deviatoric plastic strains ε_{d50}^p and ε_{d95}^p can thus be determined. Finally, substituting the obtained deviatoric plastic strains ε_{d50}^p and ε_{d95}^p into Eq. (15) corresponding to M=0.5 and M=0.95 respectively, the hardening parameters n and γ required by the proposed model can

be obtained. The comparison between the hyperbolic relationship and GNL hardening law of the proposed model is shown in Fig. 2.

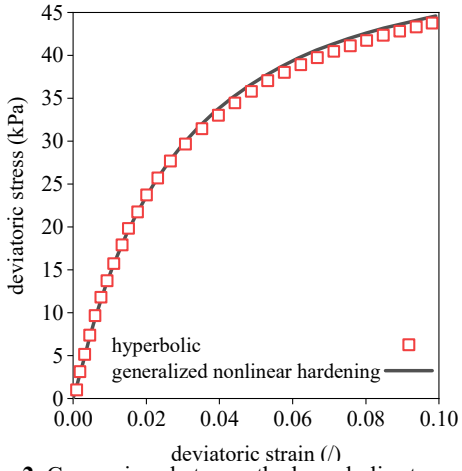

Figure 2. Comparison between the hyperbolic stress-strain relationship and that computed by proposed constitutive model.

As shown in Fig. 2, the generalized non-linear (GNL) hardening law of the proposed model can reasonably represent the hyperbolic response under specific condition. Moreover, by adjusting the value of parameter n (noticing that parameter may also changes according to Eq. (17) when the deviatoric plastic strains is determined), the generalized non-linear (GNL) hardening law can describe versatile stress-strain relations, as shown in Fig. 3:

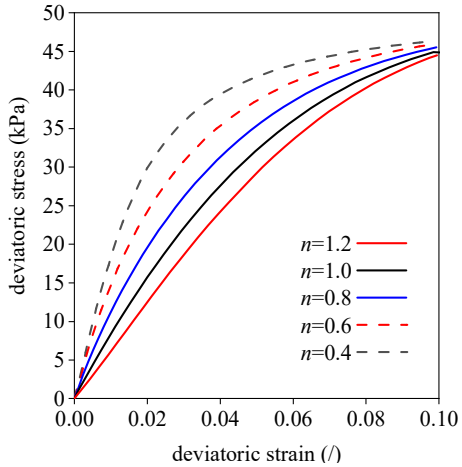

Figure 3. Various stress-strain relationship curves given by the generalized non-linear (GNL) hardening rule.

4. Simulation of soil element tests and centrifuge test

The performance of the proposed total stress constitutive model is evaluated through comparing with laboratory soil element tests (Sheu 1985) and response of cyclically-loaded monopile in centrifuge tests (Li et al. 2020) in this section. The soils used in the soil element tests and centrifuge tests are normally-consolidated (NC) Georgia clay and Malaysia kaolin clay, respectively. The model parameters for simulation are listed in Tab. 1 (where z denotes the depth below the ground surface).

Table 1. Model parameters for simulation

Parameters	Unit	Georgia clay	Malaysia kaolin clay
s_u	kPa	97	1.39z
γ	-	16.5	150
n	-	0.56	0.95
μ	-	130	10
ψ	-	1.1	1.0
G_0^{ref}	MPa	51.8	34.7
n_g	-	0.6	0.85
$\delta_{rem}(\delta_{rem}^e)$	-	0.3	0.33
$\varepsilon_{95}^p(\varepsilon_{e95}^p)$	-	1.5	1.89

4.1. Simulation of soil element tests

The soils used in the soil element tests are normally-consolidated (NC) Georgia clay (Sheu 1985). Accordingly, these tests are designated as CIU triaxial compression (CIU-TXC) tests and CIU cyclic triaxial tests.

Figure 4 compares the measured and simulated response of Georgia kaolin clay from CIUTC tests. It is seen that the proposed model can well represent the initial modulus and ultimate capacity of the measured curve, and the general stress-strain relationship is also reasonably simulated.

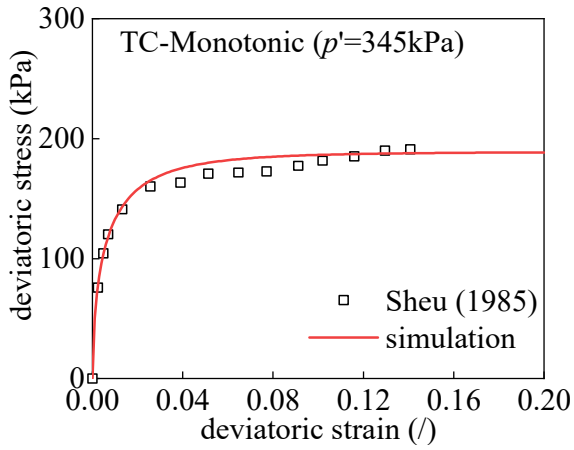

Figure 4. Measured and simulated response of Georgia kaolin clay from CIU-TXC test.

Figure 5 (a) and (b) show the measured response of Georgia kaolin clay from two CIU cyclic triaxial tests where cyclic deviatoric stress q_{cyc}=136 kPa and 140 kPa, respectively. And Figure 5 (c) and (d) represent the results calculated by the proposed model. It is seen that the proposed mode can reasonably represent the ratcheting effect (i.e., the axial strains at the peak deviatoric stress gradually grows with the increase of cycles). In addition, the proposed model can also simulate the trend that the hysteresis loop expands and rotates under repeated cyclic loading. However, the proposed model tends to over-estimate the rate of stiffness degradation following unloading.

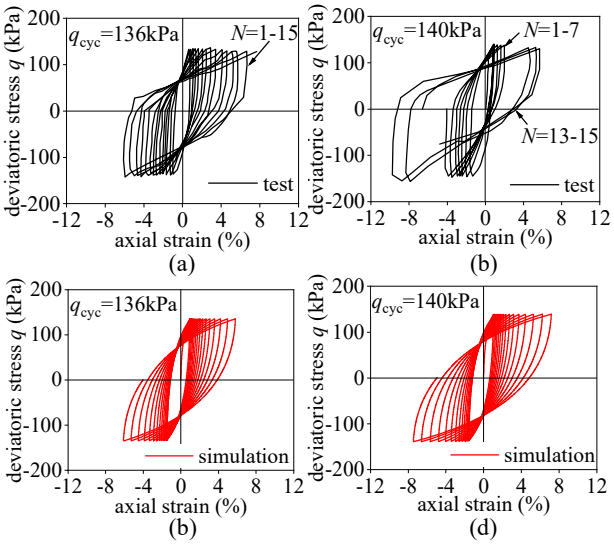

Figure 5. Measured and simulated response of Georgia kaolin clay from CIU cyclic triaxial tests: (a)-(b) test data; (c)-(d) model simulation

4.2. Simulation of cyclic loaded piles in centrifuge tests

To illustrate the application of the proposed model to simulate the response of monopile foundation in undrained clay under cyclic lateral loading, two centrifuge tests performed by Li et al. (2020) are modeled through finite element analysis (FEA). Furthermore, the parameters of the proposed model are calibrated by simulating the undrained triaxial cyclic tests of Malaysia kaolin clay performed by Ho (2013), which adopts the same soil with the centrifuge tests above (see Fig. 6).

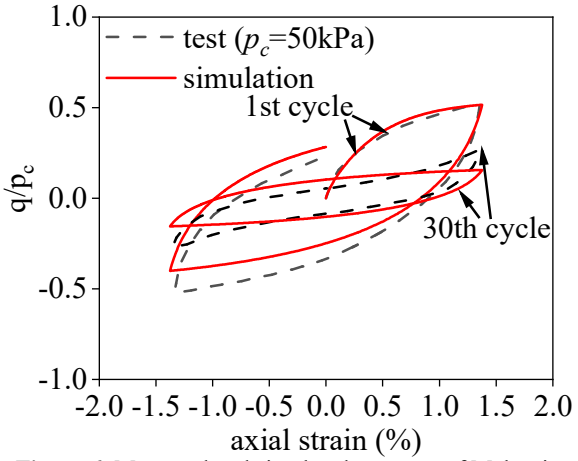

Figure 6. Measured and simulated response of Malaysia kaolin clay from CIU cyclic triaxial tests.

The numerical analysis is performed by using ABAQUS code. Figure 7 shows the FE mesh used in analyzing the monopile response of centrifuge tests. The model pile has an aspect ratio of L/D =24 (where L and D denotes the embedment length and diameter of the model pile, respectively). Due to the symmetric feature of the problem, only half domain is modeled. The boundary extends about 15D and 8D from the edge of the model, which is sufficient to eliminate the boundary effect (Li et al. 2020). In addition, the cyclic loading is exerted by applying a uniform lateral displacement u at the pile head, which is about 2D above the ground surface.

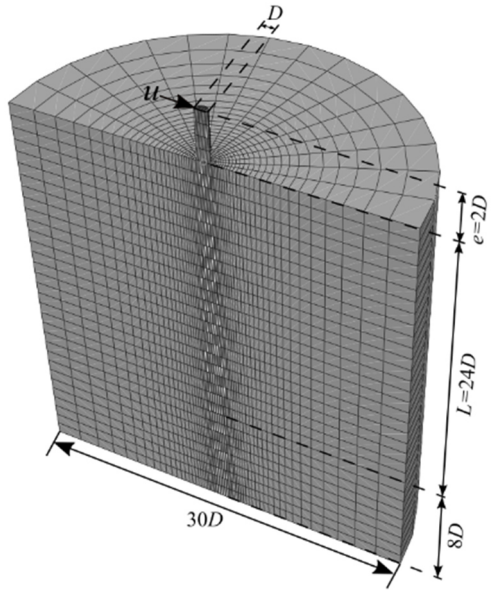

Figure 7. FE mesh used in simulating the response of free-head monopile under cyclic loading.

Figure 8 presents the measured and computed normalized load-displacement curve of pile head with different loading amplitudes. It is seen that the normalized peak load of each cycle gradually decreases due to softening of the undrained shear strength and stiffness of soil around the monopile foundation. Generally, the proposed model can reasonably represent this trend. However, the results computed by the proposed model tend to slightly overestimate the load on the monopile foundation at peak displacements.

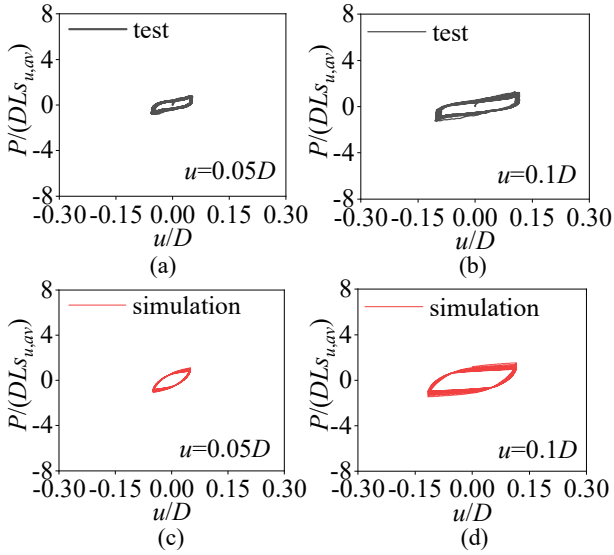

Figure 8. Measured and simulated normalized load–displacement response of monopile foundation: (a)-(b) test data; (c)-(d) model simulation. ($s_{u,av}$ denotes the average undrained shear strength along the embedment length L below the ground surface)

5. Conclusions

A total stress-based constitutive model is presented for cyclically loaded undrained clay, with the purpose of analyzing the response of foundations supporting offshore wind turbines (OWT). For this purpose, a generalized non-linear (GNL) hardening law combined with bounding surface plasticity is proposed to make the total stress-based model that was initially proposed for metals suitable for clayey soils. The model is used to simulate a series of soil element tests of different types of undrained clay and applied to analyze the response of monopile foundations in cyclic loading centrifuge model tests. The following conclusions can be drawn from this work:

- The generalized non-linear (GNL) hardening law can represent versatile stress-strain relations of undrained clays.
- The proposed model can reasonably capture the behavior of undrained clays under monotonic and cyclic loading.
- Numerical analysis based on the proposed model can reasonably reproduce OWT foundation loading-displacement hysteresis and the decrease in foundation stiffness during cyclic loading.

Lastly, it should be noted that due to the adopted total stress-based framework, the generation and dissipation of excess pore pressure during cyclic loading is not explicitly considered. When the latter response is critical for engineering application, effective stress-based models should be considered.

Acknowledgements

The authors are grateful for the financial support provided by National Natural Science Foundation of China under Grant Nos. 41902278 and 51738010.

References

Achmus, M., Kuo, Y. -S., Abdel-Rahman, K. "Behavior of monopile foundations under cyclic lateral load." Computers and Geotechnics, 36(5), pp. 725-735, 2009. https://doi.org/10.1016/j.compgeo.2008.12.003

Anastasopoulos, I., Gelagoti, F., Kourkoulis, R., Gazetas, G. "Simplified Constitutive Model for Simulation of Cyclic Response of Shallow Foundations: Validation against Laboratory Tests." Journal of Geotechnical and Geoenvironmental Engineering, 137(12), pp. 1154-1168, 2011. https://doi.org/10.1061/(ASCE)GT.1943-5606.0000534

Bourgeois, E., Rakotonindriana, M. H. J., Le Kouby, A., Mestat, P., Serratrice, J. F. "Three-dimensional numerical modelling of the behaviour of a pile subjected to cyclic lateral loading." Computers and Geotechnics, 37(7-8), pp. 999-1007, 2010. https://doi.org/10.1016/j.compgeo.2010.08.008

Byrne, B. W., Houlsby, G. T., Burd, H. J., Gavin, K. G., Igoe, D. J. P., Jardine, R. J., Martin, C. M., McAdam, R. A., Potts, D. M., Taborda, D. M. G., Zdravković, L. "PISA design model for monopiles for offshore wind turbines: application to a stiff glacial clay till." Géotechnique 70(11), pp. 1030-1047, 2020. https://doi.org/10.1680/jgeot.18.P.255

Dafalias, Y. F. "Bounding surface plasticity. I: Mathematical foundation and hypoplasticity." Journal of engineering mechanics, 112(9), pp. 966-987, 1986. https://doi.org/10.1061/(ASCE)0733-9399(1986)112:9(966)

Einav, I., Randolph, M. F. "Combining upper bound and strain path methods for evaluating penetration resistance." International Journal for Numerical Methods in Engineering, 63(14), pp. 1991-2016, 2005. https://doi.org/10.1002/nme.1350

Hardin, B. O. "The nature of stress-strain behavior for soils." In: Earthquake Engineering and Soil Dynamics--Proceedings of the ASCE Geotechnical Engineering Division Specialty Conference, Pasadena, California, 1978, pp. 19-21.

Ho, J. "Cyclic and post-cyclic behaviour of soft clays." Ph.D. thesis, National University of Singapore, 2013.

Hong, Y., He, B., Wang, L. Z., Wang, Z., Ng, C. W. W., Mašín, D. "Cyclic lateral response and failure mechanisms of semi-rigid pile in soft clay: centrifuge tests and numerical modelling." Canadian geotechnical journal, 54 (6), pp. 806-824, 2017. https://doi.org/10.1139/cgj-2016-0356

Houlsby, G. 1999. "A model for the variable stiffness of undrained clay." In: Proc. Int. Symp. on Pre-Failure Deformation Characteristics of Soils, Turin, Italy, 1999, pp. 443-450.

Huang, M., Liu, L., Shi, Z., Li, S. "Modeling of laterally cyclic loaded monopile foundation by anisotropic undrained clay model." Ocean Engineering, 228, 108915, 2021. https://doi.org/10.1016/j.oceaneng.2021.108915

Kondner, R. L. "Hyperbolic stress-strain response: cohesive soils." Journal of the Soil Mechanics and Foundations Division, 89 (1), pp. 115-143, 1963. https://doi.org/10.1061/JSFEAQ.0000479

Kourkoulis, R., Lekkakis, P., Gelagoti, F., Kaynia, A. "Suction caisson foundations for offshore wind turbines subjected to wave and earthquake loading: effect of soil–foundation interface." Géotechnique, 64 (3), pp. 171-185, 2014. https://doi.org/10.1680/geot.12.P.179

Krabbenhøft, K., Galindo-Torres, S. A., Zhang, X., Krabbenhøft, J. "AUS: Anisotropic undrained shear strength model for clays." International Journal for Numerical and Analytical Methods in Geomechanics, 43 (17), pp. 2652-2666, 2019. https://doi.org/10.1002/nag.2990

Li, S., Yu, J., Huang, M., Leung, C. F. "Application of T-EMSD based p-y curves in the three-dimensional analysis of laterally loaded pile in undrained clay." Ocean Engineering, 206, 107256, 2020. https://doi.org/10.1016/j.oceaneng.2020.107256

Liu, B., Zhang, Y., Ma, Z., Andersen, K. H., Jostad, H. P., Liu, D., Pei, A. "Design considerations of suction caisson foundations for offshore wind turbines in Southern China." Applied Ocean Research, 104, 102358, 2020. https://doi.org/10.1016/j.apor.2020.102358

Nanda, S., Arthur, I., Sivakumar, V., Donohue, S., Bradshaw, A., Keltai, R., Gavin, K., Mackinnon, P., Rankin, B., Glynn, D. "Monopiles subjected to uni- and multi-lateral cyclic loading." Proceedings of the Institution of Civil Engineers - Geotechnical Engineering, 170 (3), pp. 246-258, 2017. https://doi.org/10.1680/jgeen.16.00110

Seidalinov, G., Taiebat, M. "Bounding surface SANICLAY plasticity model for cyclic clay behavior." International Journal for Numerical and Analytical Methods in Geomechanics, 38 (7), pp. 702-724, 2014. https://doi.org/10.1002/nag.2229

Sheu, W. -Y. "Modeling of stress-strain-strength behavior of a clay under cyclic loading" Ph.D. thesis, University of Colorado, 1985.

Shi, Z., Finno, R. J., Buscarnera, G. "A hybrid plastic flow rule for cyclically loaded clay." Computers and Geotechnics,

101, pp. 65-79, 2018. https://doi.org/10.1016/j.compgeo.2018.04.018

Subramaniam, P., Banerjee, S. "A correction to damping ratio for hyperbolic–hysteretic model for clayey soil." International Journal of Geotechnical Engineering, 7 (2), pp. 124-129, 2013. https://doi.org/10.1179/1938636213Z.00000000025

Whyte, S. A., Burd, H. J., Martin, C. M., Rattley, M. J. "Formulation and implementation of a practical multi-surface soil plasticity model." Computers and Geotechnics, 117, 103092, 2020. https://doi.org/10.1016/j.compgeo.2019.05.007

Zhang, Y., Andersen, K. H. "Scaling of lateral pile p - y response in clay from laboratory stress-strain curves." Marine Structures, 53, pp. 124-135, 2017. https://doi.org/10.1016/j.marstruc.2017.02.002

Zhu, J., Yu, J., Huang, M., Shi, Z., Shen, K. "Inclusion of small-strain stiffness in monotonic p-y curves for laterally loaded piles in clay." Computers and Geotechnics, 150, 104902, 2022. https://doi.org/10.1016/j.compgeo.2022.104902·